Contrib Mineral Petrol (1987) 97:320–332

Contributions to Mineralogy and Petrology

Water solubility in aluminosilicate melts

Paul F. McMillan and John R. Holloway
Departments of Chemistry and Geology, Arizona State University, Tempe, AZ 85287, USA

Abstract. We have compiled water solubility data for a wide range of natural and synthetic aluminosilicate melts in a search for correlations between melt composition and solubility. The published data reveal some interesting systematics. For example, molar water solubility increases with decreasing silica content in binary and pseudobinary silicates, and much higher solubilities are associated with alkali systems compared to alkaline earth silicate melts. Water solubility increases regularly with decreasing silica content along the silica-nepheline join. From the limited data available for potassium and calcium aluminosilicate melts, these systems appear to behave differently to sodium aluminosilicates. The compiled data are not nearly extensive enough to begin to understand the effects of melt composition on solubility. We suggest that many more systematic studies for a wide range of aluminosilicate melts will be necessary before we can systematize and understand the compositional dependence of water solubility. We have also examined results of experiments designed to probe the details of the water dissolution mechanism, and discuss the present state of interpretation of these data. We conclude that although considerable progress has been made, the water dissolution process is still not well understood at the molecular level, and remains an important research problem.

Introduction

Water is generally recognized as the most important magmatic volatile species, both for its abundance and for its effects on melt properties and crystal-melt phase relations, hence it is important to understand both the thermodynamics and the mechanisms of silicate melt-water interactions. A number of studies have been carried out to determine the extent of water solubility in aluminosilicate melts as a function of pressure, temperature, and melt composition. At the present time, there seems to be a general perception within a large part of the geological community that water solubility is "understood", with detailed models for both the thermodynamic (Burnham 1981) and the physical (Mysen 1983) nature of the process, yet even a cursory examination of the literature shows that this cannot be the case. For example, Burnham's (1975a, b; 1981; Eggler and Burnham 1984) well-known thermodynamic models for water solubility are essentially based on a dissolution mechanism involving complete dissociation of H_2O on reaction with the melt. However Stolper (1982a, b) has shown via infrared spectroscopic measurements that much of the water dissolves as molecular H_2O over most of the pressure range. Stolper has developed an alternative and equally successful thermodynamic model for water dissolution based on the results of his infrared work, with only partial dissociation of H_2O (Stolper 1982a; Silver and Stolper 1985). The sophisticated structural models of Mysen and co-workers (Mysen and Virgo 1980; 1986a, b; Mysen et al. 1980; Mysen 1983) are based heavily on particular detailed assignments of Raman spectral data, which may be open to other, alternative interpretations (McMillan 1984). The thermodynamic model of Burnham (1981) invokes a suite of "quasi-crystalline" thermodynamic components as mixing species in hydrous and anhydrous aluminosilicate melts, which Burnham (1981) considers to have real structural significance. There is no direct structural evidence for the existence of melt species with the stoichiometry or geometry assumed by Burnham (1981). This in itself would not negate the thermodynamic model, since thermodynamic components need not have actual structural significance, but Burnham (1981) also bases part of his philosophy on the premise that the equimolal, isothermal, isobaric solubilities of H_2O in $NaAlSi_3O_8$, $KAlSi_3O_8$ and $CaAl_2Si_2O_8$ melts are essentially the same. This is known not to be the case (Oxtoby and Hamilton 1978b; Voigt et al. 1981; this work, Fig. 6). Finally, although there are known to be wide variations in water solubility between different silicate and aluminosilicate melts (Oxtoby and Hamilton 1978a, b; Dingwell et al. 1984; Silver and Stolper 1985; this work) there is no good model for the effect of melt composition on water dissolution. Burnham (1974, 1975a) suggested an empirical calculation scheme to take account of melt composition based on his water dissolution model, but predicted water solubilities do not agree well with experiment for many simple melt compositions (Oxtoby and Hamilton 1978a; Voigt et al. 1981; McMillan and Holloway 1983) or for natural granitic or phonolitic compositions (Dingwell et al. 1984).

In view of these contradictions and inadequacies, we decided to examine the present state of understanding of water dissolution in aluminosilicate melts. We have compiled results of previous water solubility investigations to investigate any systematic variation in water solubility with melt composition. The data do reveal some systematic behaviour, but they are insufficient to establish detailed correlations. We have also examined the current under-

Offprint requests to: P.F. McMillan

standing of the mechanism for water dissolution, mainly gained from spectroscopic experiments on the hydrous glass or melt. Again, these experiments have given considerable insight into the nature of melt-water interactions, but the problems are far from resolved. We conclude that studies of water dissolution in aluminosilicate melts remain an worthwhile and important area of active research, and this review serves to highlight areas where further experimental work is needed.

Water solubility determination

The methods used to determine water solubility can have a large effect on the solubility data obtained. Specific techniques used to determine H_2O solubility in aluminosilicate melts include (a) the presence or absence of excess fluid pits in charges of known total water content, (b) variation of liquidus temperature as a function of H_2O content, (c) various methods of bulk analysis of glass quenched from the hydrous melt, (d) weight loss of the capsule + sample assembly at 110° C, (e) weight loss at higher temperature (1000–1200° C), and (f) microbeam analysis of quenched hydrous glass by micro-infrared or ion beam spectrometry. These techniques fall into two broad classes: phase equilibrium experiments (a and b), and analysis of quenched glasses (c–f).

Method (a) has been used for melts of albite and granitic compositions (Burnham and Jahns 1962). In this case, capsules with different sample/water ratio are run at constant pressure and temperature. Water-oversaturated samples contain vesicles of aqueous fluid, many of which are located at the capsule-melt interface. Isobaric quenching results in a large decrease in the volume of the fluid, and the external pressure forces the capsule metal into the vesicles, creating dimples or pits in the external surface of the capsule. This is an accurate technique for determining water content in the melt and is not subject to the problems discussed below for quench techniques, but has a low precision, in the range of ± 0.5 to ± 1 wt% H_2O. Method (b) is similar, but relies on the presence or absence of a liquidus crystalline phase to fix H_2O solubility. This method has been used by a number of workers (Yoder 1965; Eggler 1973; Hodges 1973, 1974) to investigate water solubilities at very high H_2O contents, and is subject to approximately the same imprecision as the dimple method (a). In addition to being relatively imprecise, method (a) does not work well with iron-containing samples. Hamilton et al. (1964) suggested that this is because oxidation of ferrous iron by H_2O during the run consumes some of the H_2O, resulting in over-estimation of the water solubility in the melt. A further problem in this case is that the H_2 gas formed by this redox reaction causes dimples in the charges.

Methods (c) involve grinding the quenched glass to approximately 80 mesh before analysis. The results obtained often agree with those from methods (d) and (e) for lower pressure runs, but at high pressures (above around five kbars), the H_2O contents determined with method (c) are much lower, which can be attributed to loss of water during the grinding process. The precision of method (c) can be quite high, close to ± 0.1 wt% H_2O.

In method (d), the amount of H_2O remaining in the fluid is measured, and so gives the amount dissolved as the difference between that originally weighed into the capsule, and the weight loss observed at 110° C. This is a commonly used technique, and consistently gives good results. With iron-bearing samples, the amount of H_2O used up in oxidation of ferrous iron must be calculated from analyses of the starting material and the run products. Methods (d) and (e) can be used together, and should yield consistent results. Since dissolved H_2O can react with ferrous iron in the sample during the 1000° C heating process, it is necessary to analyze iron-bearing samples before and after heating.

Other fundamental problems are associated with all of the analysis methods in addition to iron oxidation. Techniques (c–f) require that the H_2O content of the quenched glass be the same as the melt at pressure and temperature. Analytical techniques relying on analysis of the bulk glass also require that the glass is free of vesicles containing H_2O from the fluid phase. There are several instance where these criteria may not be met.

One major problem is posed by the occurrence of fluid inclusions in the sample. These can be formed during the run, or during the quench for high water content (above 6–9 wt%) samples. Inclusions are commonly formed during the run when the starting material is in powder form. In low viscosity melts, these migrate out of the melt during the run, and do not pose a problem. In high viscosity melts, the inclusions remain in the melt, unless the melt is held far above its liquidus for an extended period of time. The number of inclusions, and consequently the apparent solubility, increases with decreasing particle size of the starting material (Tuttle and Bowen 1958, p 14). The best way to measure water solubility in high viscosity melts is to first prepare a bubble-free glass sample as the starting material by melting under vacuum, then break the glass into millimetre-size pieces and saturate them by diffusing water into them. This prevents formation of inclusions during the run, so that any inclusions present will have formed during the quench. Since these vesicles represent water which was dissolved in the melt at pressure and temperature, it is important to include their contribution in the water analysis. This can be done by heating the sample in a thermo-gravimetric balance in which weight loss is followed as a function of heating time and temperature, and summing all weight loss contributions. For samples which do not form fluid inclusions on quenching, in-situ analysis of H_2O can be done via micro-infrared spectrometry (Stolper 1982b), or ion microprobe analysis for H (Karsten et al. 1982). Melts containing more than 8–10 wt% H_2O lose water both during and after the quench (Kadik and Lebedev 1968). This water loss is of two types; formation of vesicles during the quench, and diffusion of water out of the glass. The former can be accounted for as discussed above, but the loss by diffusion is very difficult to treat, and makes water solubility determination at very high H_2O contents only possible via phase equilibrium techniques (see discussion below of albite solubility data as a function of temperature). Finally, we note that low viscosity melts often do not quench to glasses. The resulting mixture of crystals and glass usually contains considerably less water than the melt at pressure and temperature, and so all analytical methods for such samples are useless.

Other discussions of the techniques for measuring water solubility in silicate melts are found in Burnham and Jahns (1962), Hamilton et al. (1964), Dingwell et al. (1984), and Hamilton and Oxtoby (1986).

The effect of pressure

"Square root relationships"

It has long been known that the maximum water solubility in a given silicate melt increases with increasing water pressure (Goranson 1931). A number of workers in the glass sciences conducted isobaric water solubility experiments on silicate melts and glasses near one atmosphere total pressure, and found that water solubility varied as the square root of the partial pressure of water vapour (Tomlinson 1956; Russell 1957). This observation was used by these and other authors to support a water dissolution model involving dissociation of H_2O into two hydroxylated species in the glass or melt. The same reasoning was later applied to solubility data obtained at higher pressures (Hamilton et al. 1964; Hodges 1974), and it has become customary to plot water solubilities in silicate melts versus the square root of water pressure or fugacity in the fluid (Hodges 1974; Oxtoby and Hamilton 1978a; Dingwell et al. 1984). In these plots, a linear relation between the solubility and the square root of water pressure or fugacity in the fluid ($p_{H_2O}^{1/2}$ or $f_{H_2O}^{1/2}$) is taken as support for a water dissolution mechanism involving dissociation of H_2O (Mysen 1977; Eggler and Ro-

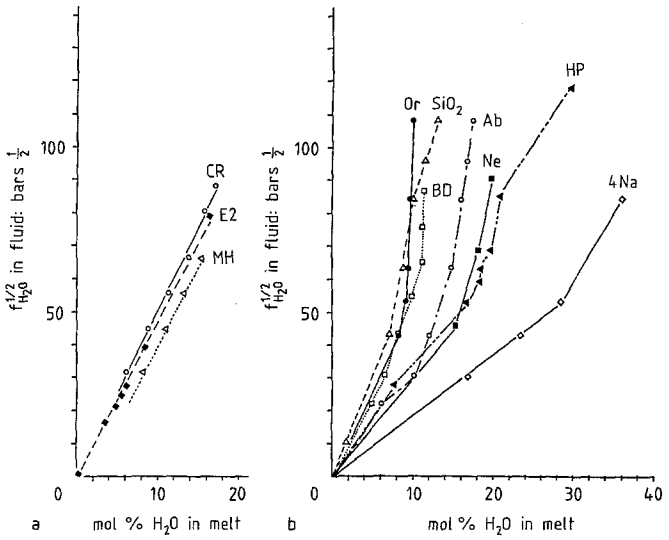

Fig. 1a, b. Plots of square root of water fugacity in fluid versus molar water solubility in melt. **a** Three compositions which show linear root fugacity-water solubility relations. **b** Several which do not. *CR* Columbia River basalt; *MH* Mount Hood andesite (Hamilton et al. 1964); *E2* CaO 0.26, Al_2O_3 0.09, SiO_2 0.65 (McMillan et al. 1986); *SiO_2* (Kennedy et al. 1962); *Or* $KAlSi_3O_8$; *Ab* $NaAlSi_3O_8$; *Ne* $NaAlSiO_4$; *4Na* Na_2O 0.36 Al_2O_3 0.09 SiO_2 0.55; *BD* Beinn and Dubhaich granite (Oxtoby and Hamilton 1978a, b, d); *HP* Harding pegmatite (Burnham and Jahns 1962)

senhauer 1978). However, such high pressure solubility measurements are carried out as a function of varying total pressure, and give polybaric points on the water saturation surface. Any equilibrium expression for the water dissolution reaction along the saturation boundary must contain a pressure dependent exponential term involving the change in partial molar volumes of the reacting species (Goranson 1937; Wasserburg 1957; Stolper 1982a; McMillan et al. 1986). For such polybaric data, no linear relationship between water solubility and the square root of pressure or water fugacity should be expected, irrespective of the dissolution reaction. Hamilton et al. (1964) and McMillan et al. (1986) did find linear relationships between solubility and $f_{H_2O}^{1/2}$ for three aluminosilicate melt compositions (Fig. 1a), although the bulk of synthetic and natural aluminosilicate melts do not show any such linear relation (Fig. 1b). The molar water solubilities described in this Figure and throughout this paper are given on a one-oxygen basis, i.e., using a molecular weight for the dry melt normalized to one mole of oxygen atoms. This was done to report the water solubilities within the pseudo-binary system H_2O-M_xO, where M_x refers to all cations in the dry melt composition. The above discussion suggests that the observed linear relations between solubility and $f_{H_2O}^{1/2}$ for three unrelated aluminosilicate compositions are entirely fortuitous.

In their plots of water solubility versus $p_{H_2O}^{1/2}$ or $f_{H_2O}^{1/2}$, Hodges (1974) and Oxtoby and Hamilton (1978a) considered that their data represented linear regions separated by breaks in slope, indicative of some change in water solubility mechanism. In fact, the data of Hodges (1974) and Oxtoby and Hamilton (1978a) do not require discrete linear portions, but could be as well fit by curves with continuously changing slope, which need not directly reflect any changes in the mechanism for water dissolution. These continuous slope changes are most probably due to variations in either the partial molar volumes of the aqueous fluid or the hydrous melt species as a function of pressure, which could be associated with changes in the dissolution reaction, but not necessarily so.

"Burnham models"

Burnham and Davis (1971, 1974) used the results of their P–V–T measurements on the system $NaAlSi_3O_8-H_2O$ (the albite used was a natural sample, close to Ab_{85}) to construct isobaric sections relating the activity of water in the fluid and the mole fraction of water dissolved in the melt [$X(H_2O)$, using Burnham's eight-oxygen basis for the dry melt]. These authors suggested that, for $X(H_2O)$ less than 0.5, there was a linear relationship between water activity and the square of the mole fraction of dissolved water $[X(H_2O)]^2$, with small positive deviations from this relation at higher water contents. These workers then used these observations to construct their well-known models for water dissolution in silicate melts, involving association and dissociation reactions of hydrous species in the melt, and the associated activity-composition relationships for hydrous melts (e.g., Burnham 1974; 1975a, b; 1981; Eggler and Burnham 1984; Burnham and Nevkasil 1986). The success of this family of models as applied to multi-component aluminosilicate systems has contributed greatly to the general perception that the mechanism for water dissolution in silicate melts is "understood" in both a physical and a thermodynamic sense. However, the actual P–V–T data obtained by Burnham and Davis (1971) were for only three compositions; with water contents of 5.86, 8.25 and 10.90 wt%, corresponding to mole fractions of 0.47, 0.57 and 0.64 respectively. Burnham and Davis (1971) apparently did not use the results for the 5.86 wt% sample due to the presence of crystals in the charges, so the P–V–T data presented concerned only the 8.25 and 10.90 wt% samples, with $X(H_2O)$ of 0.57 and 0.64. For the dry melt [$X(H_2O)=0$], Burnham and Davis (1971) estimated the P–V–T relations for dry albite melt from specific volume measurements on dry glass at 1 bar and 20° C coupled with thermal expansion data for the glass from Orlowski and Koenig (1941), and from the compressibility of crystalline albite, assuming that the glass would be 10% more compressible than the crystal. The mean isothermal specific volume isobars as a function of water content of the melt were then drawn as linear functions to fit the data points at $X(H_2O)=0.57$ and 0.64 and the estimated points at $X(H_2O)=0$ (Figs. 12 and 13 of Burnham and Davis 1971). In view of the limited data set and the assumptions involved in calculating P–V–T for dry albite melt, we suggest that conclusions derived for mole fractions of water of less than 0.5 be treated with some care.

"Stolper's model"

More recently, Stolper (1982a, b) and Silver and Stolper (1985) have proposed an alternative thermodynamic model for water dissolution in aluminosilicate melts, where both hydroxyl (OH) and molecular H_2O groups are present as dissolving groups in the hydrous liquid. Both species were identified from specific combination bands in the infrared absorption spectra of hydrous glasses, and the thermodynamic model was based on the results of quantitative infra-

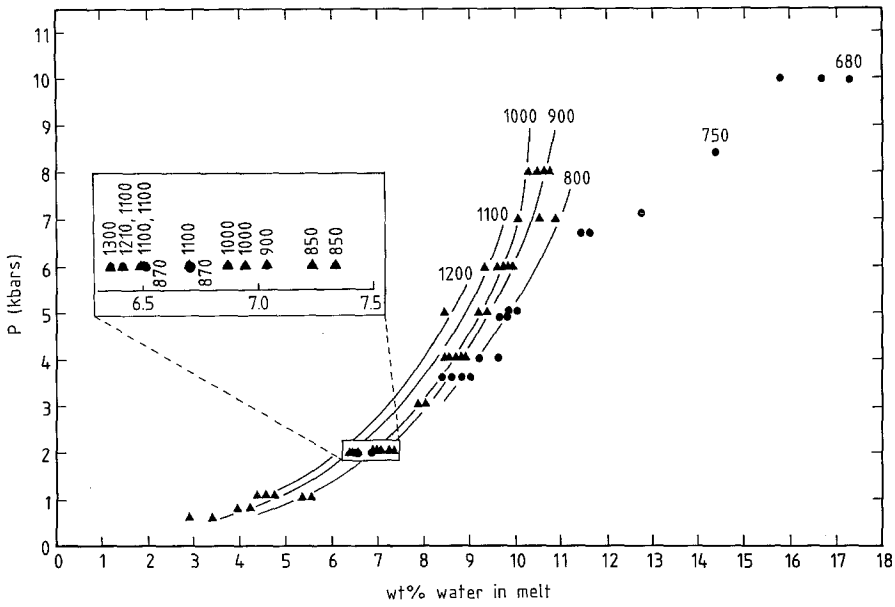

Fig. 2. Temperature dependence of water solubility in albite melt. Data shown are taken from Burnham and Jahns (1962) (●) and Hamilton and Oxtoby (1986) (▲) (also D. Hamilton, pers. comm. 1982). Isotherms have been estimated visually through the data points, although there is often considerable scatter (*inset*)

red absorption measurements. Stolper (1982a, b) showed that the molecular water was not simply present in the form of inclusions, and later studies at high temperature and pressure (Stolper et al. 1983; Aines et al. 1983) showed that the results extended to hydrous melts at high temperatures and pressures. These experiments provided the first direct observation of the dissolving species in hydrous aluminosilicate melts, and the thermodynamic model of Stolper (1982a) and Silver and Stolper (1985) is more physically satisfying than that of Burnham and co-workers, since it is based on a wider range of data, and on direct physical measurements of the hydroxylated species. It is of interest to note, however, that the activity-composition relations for $NaAlSi_3O_8-H_2O$ derived using Stolper's (1982a, b) model are indistinguishable from those calculated by Burnham and Davis (1971, 1974).

The effect of temperature

In general, it has been found that water solubility decreases with increasing temperature at both high and low pressures (Mysen 1977; Coutures and Peraudeau 1981). One exception was noted by Kurkjian and Russell (1958) for SiO_2-Li_2O melts with $P(H_2O)$ near one atmosphere. However the results of these authors differ markedly from those of other workers (see Coutures and Peraudeau 1981; also Fig. 3), and the observed temperature dependency may be a strong function of other experimental conditions. Kennedy et al. (1962) also suggested an increase in solubility with increasing temperature, from their data on the system SiO_2-H_2O. In general, the magnitude of the temperature coefficient of water solubility is small when compared with the effect of pressure on solubility.

Solubility results for albite melt as a function of temperature, taken from Burnham and Jahns (1962), and from the work of S. Oxtoby (Oxtoby and Hamilton 1978a; D. Hamilton, pers. comm. 1982; Hamilton and Oxtoby 1986), are compared in Fig. 2. Below around five kbars total pressure, the two data sets overlap, and a small negative temperature dependence of water solubility is apparent. This is in agreement with the results of Kadik and Lebedev (1968). Above this pressure, which corresponds to a water content of around 9 wt%, the two data sets diverge considerably. The rate of increase in solubility with pressure decreases markedly for the data of Oxtoby and Hamilton, while the data of Burnham and Jahns (1962) below 800° C continue to show a regular increase in solubility with pressure. Kadik and Lebedev (1968) have discussed the difficulty in obtaining reliable water contents in albite melt above a total water content of 8–10 wt%. Their results indicated that above this water content, the melt does not retain its dissolved water content, but a large amount is released as bubbles during the quench. This suggests that quench experiments cannot be used to obtain reliable water solubilities for high water contents in the melt, and that phase equilibrium determinations [methods (a) and (b) discussed above] must be used. Since the data of Burnham and Jahns (1962) were obtained using the dimple technique, while those of Oxtoby and Hamilton were measured on quenched samples, the former are more reliable above around 5 kbars. Since the data of Burnham and Jahns (1962) were restricted to temperatures of 700–800° C above this pressure, we currently have no reliable solubility data for albite melts at high pressures and temperatures.

The effects of composition

Low pressure data

Coutures and Peraudeau (1981) have recently summarized the results of water solubility measurements on silicate melts and glasses at low pressure, near one atmosphere. Data are available for simple alkali and alkaline earth silicate systems which give an indication of the effect of silica content on water solubility. Several studies have been carried out for the binary alkali silicate systems SiO_2-Li_2O, SiO_2-Na_2O and SiO_2-K_2O at low pressure. There is considerable disagreement between these studies, and the results of any single study can not be considered reliable (see Coutures and Peraudeau 1981). However, there are some general similarities in the variation of water solubility with silica content within these systems, which are useful to ex-

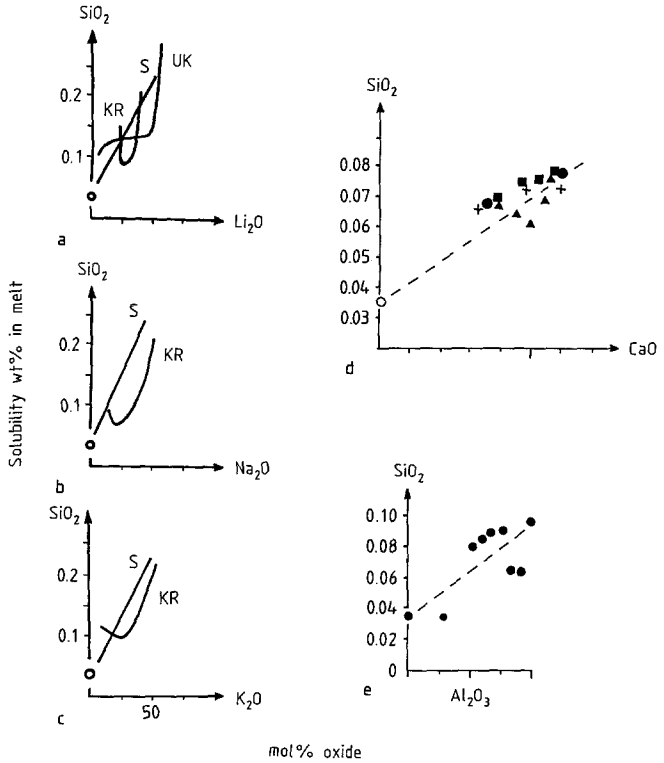

Fig. 3a–e. Water solubilities in binary silicate melts at or near one atmosphere. **a** SiO_2-Li_2O; **b** SiO_2-Na_2O; **c** SiO_2-K_2O; **d** SiO_2-CaO; **e** $SiO_2-Al_2O_3$. Data for alkali silicates are at one atmosphere and near 1500° C; data for SiO_2-CaO are at one atmosphere and 1500–1600° C; data for $SiO_2-Al_2O_3$ are at 0.83 atmosphere and 1700–2000° C. Curves for the alkali silicates are redrawn from Coutures and Peraudeau (1981). *S* Scholze et al. (1962); *UK* Uys and King (1963); *KR* Kurkjian and Russell (1958). Data for SiO_2-CaO are from Walsh et al. (1956) (*circles*), Iguchi and Fuwa (1970) and Iguchi et al. (1969) (*triangles*), Devauchelle (1978) (*crosses*) and Sachdev et al. (1972) (*squares*). Data for $SiO_2-Al_2O_3$ are from Coutures et al. (1980)

amine. Water solubility data for SiO_2-Li_2O, SiO_2-Na_2O and SiO_2-K_2O melts at near 1500° C and one atmosphere pressure are shown in Fig. 3(a–c). The value shown for pure SiO_2 is that obtained for the liquid at 1750° C (Scholze et al. 1962; 0.035 wt%): higher values (up to 0.06 wt%) have been reported in the glass at lower temperatures (Coutures and Peraudeau 1981). The general trend within these data is for water solubility to increase markedly with decreasing silica content, at least to the metasilicate composition (50 mol% silica).

Water solubilities have also been measured at near one atmosphere for liquids in the binary systems SiO_2-CaO (Coutures and Peraudeau 1981) and $SiO_2-Al_2O_3$ (Coutures et al. 1980) (Fig. 3d, e). Here again there are discrepancies between different data sets, and possibly suspect variations in water solubility with silica content due to experimental difficulties. For example, it is likely that the complex variations in water solubility found by Coutures et al. (1980) for $SiO_2-Al_2O_3$ melts (Fig. 3e) were at least partly due to surface tension effects in the liquid and deposition of material on the walls of the reaction vessel (G. Peraudeau, personal communication 1980). However it may be recognized from the general form of the solubility data that water solubility again increases with decreasing silica content for both these series, although to a lesser extent than for the alkali silicates (Fig. 3).

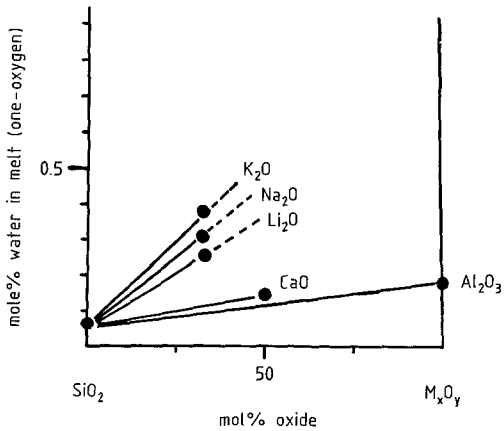

Fig. 4. Molar water solubilities (one oxygen basis) for binary silicate melts at or near one atmosphere. Molar solubilities are estimated from data in Fig. 3 (see text)

To better visualize the effect of changing metal cation on the water solubility in these simple systems, we have made a number of approximations and simplifications. For each of the above data sets, the variation in water solubility with silica content was approximated by a straight line indicating the general trend of the data (Fig. 3). An "average" value for the water solubility was then read off this line, at 67 mol% silica for the alkali silicate systems and at 50 mol% silica for SiO_2-CaO. The molar water solubility in pure Al_2O_3 melt was taken as the measured value of Coutures et al. (1980). These approximate average solubilities were then recast on a one-oxygen molar basis (Fig. 4). Within the limits of the data sets, it seems (a) that the molar water solubility in SiO_2-K_2O, SiO_2-Na_2O, SiO_2-Li_2O, SiO_2-CaO and $SiO_2-Al_2O_3$ melts increases with decreasing silica content, and (b) that water solubility in alkali silicate melts is much greater than in calcium silicate or $SiO_2-Al_2O_3$ melts. From the admittedly crude comparisons in Fig. 4, we suggest that the effect of particular components on increasing water solubility might follow the sequence

$$K_2O > Na_2O > Li_2O \gg CaO > Al_2O_3 > SiO_2$$

for metal oxide-silica binary systems at near one atmosphere pressure. Further water solubility experiments are needed at one atmosphere and below on these and other simple silicate systems, both to remove inconsistencies in the existing data sets, and to better constrain the systematics of solubility with melt composition.

High pressure data

Solubility data for SiO_2 (Kennedy et al. 1962), $Na_2O \cdot 6SiO_2$ (6S: Oxtoby and Hamilton 1978a, b) and $CaMgSi_2O_6$ (Di: Rosenhauer and Eggler 1975; Eggler and Rosenhauer 1978) melts at higher pressures are shown in Fig. 5. At pressures below the critical point for SiO_2-H_2O (around 9 kbars at 1000° C; Kennedy et al. 1962), the molar water solubility in these "depolymerized" silicates is higher than that in molten SiO_2. This is consistent with the observation for low pressure melts that water solubility generally decreases with increasing silica content. The molar solubility in the sodium silicate melt is considerably higher than

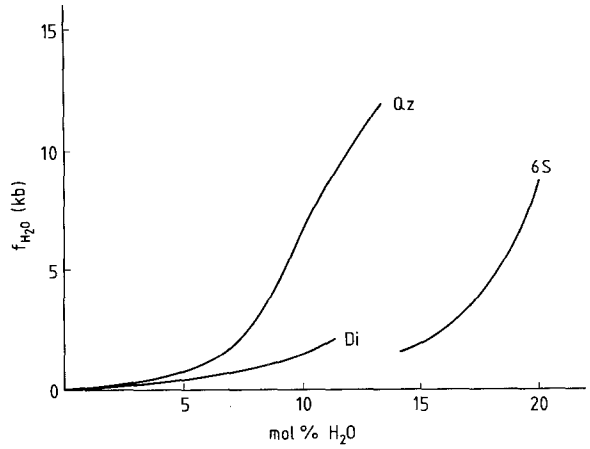

Fig. 5. Molar water solubilities (one oxygen basis) for *Qz* (SiO_2: Kennedy et al. 1962), *Di* ($CaMgSi_2O_6$: Rosenhauer and Eggler 1975; Eggler and Rosenhauer 1978) and *6S* ($Na20.6SiO_2$: Oxtoby and Hamilton 1978a, b) melts at high pressures

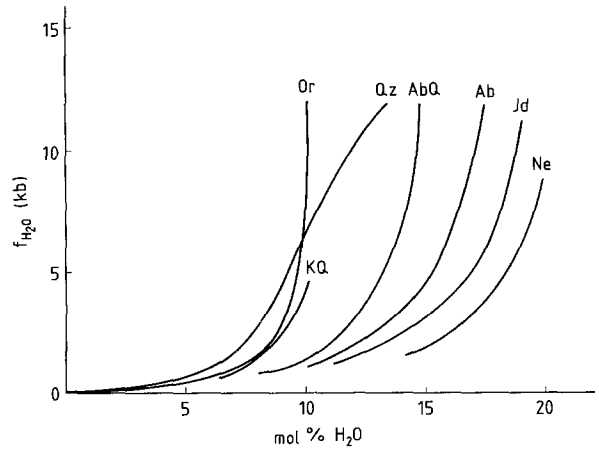

Fig. 6. Molar water solubilities (one oxygen basis) for melts along the joins $SiO_2-NaAlSiO_4$ (*Qz, AbQ, Ab, Jd, Ne*) and $SiO_2-KAlSi_3O_8$ (*Qz, KQ, Or*). Dry melt compositions are shown in Fig. 7. Data from Kennedy et al. (1962) and Oxtoby and Hamilton (1978a, b)

that in diopside melt, although the sodium silicate has much higher silica content. This suggests that the presence of Na_2O in a binary silicate melt has a larger effect on water solubility than (Ca, Mg)O. If the MgO component in the melt behaves similarly to CaO, this is consistent with the observations discussed above for one atmosphere solubilities, that molar water solubility is much higher in alkali silicate melts than in molten calcium silicates.

Solubility data for the sodium and potassium aluminosilicate joins (SiO_2-MAlO_2; M = Na, K) are summarized in Fig. 6. We note that these data, like most existing water solubility data below around 10 kbars, were obtained for quenched samples. In view of the earlier discussion of the problems inherent in quenching high water content melts (Kadik and Lebedev 1968; Fig. 2), the solubilities may be greatly underestimated above water contents of 8–10 wt% (12–13 mol% for most compositions). With this caution, there are a number of general statements which can be made regarding these solubility curves, but we suggest that

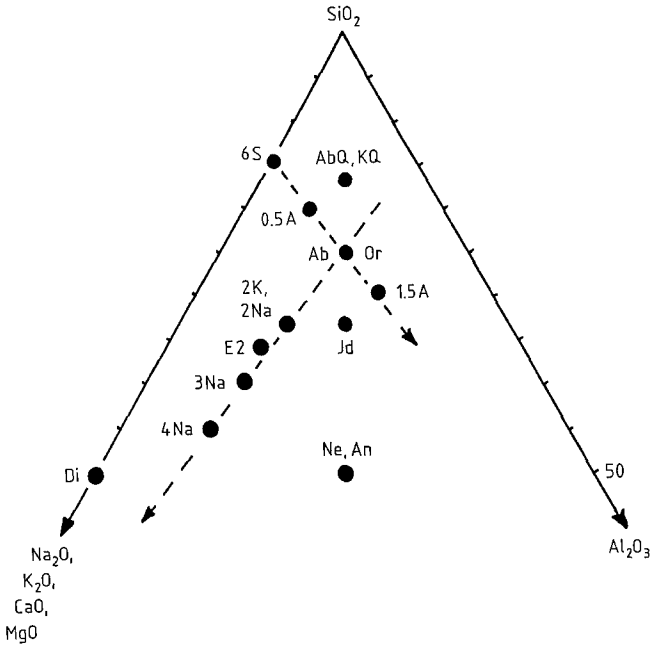

Fig. 7. Dry melt compositions for solubility curves shown in Figs. 5, 6, 8 and 9. Compositions *AbQ, Ab, Jd, Ne, 6S, 0.5A, 1.5A, 2Na, 3Na* and *4Na* (Oxtoby and Hamilton 1978a, b) lie within $Na_2O-Al_2O_3-SiO_2$; compositions *KQ, Or* and *2K* (Oxtoby and Hamilton 1978a, b) lie within $K_2O-Al_2O_3-SiO_2$; compositions *An* (Yoder 1965) and *E2* (McMillan et al. 1986) lie within $CaO-Al_2O_3-SiO_2$; *Di* (Eggler and Rosenhauer 1978) has composition $CaMgSi_2O_6$

at least some of the solubilities should be checked via phase equilibrium methods.

The data are most complete for the sodium aluminosilicate melts, and show a regular increase in molar water solubility with decreasing silica content along the $SiO_2-NaAlSiO_4$ join (Qz, AbQ, Ab, Jd, Ne: the dry melt compositions are shown in Fig. 7. We have retained the authors' original nomenclature for ease of identification within the literature source). The data for the $SiO_2-KAlSi_3O_8$ system (Oxtoby and Hamilton 1978b; Voigt et al. 1981) are more limited and show more complex behaviour. The $KAlSi_3O_8$ composition (Or) shows a low water solubility, similar to but slightly higher than pure SiO_2, for pressures below around five kbars, until the SiO_2 curve "bends over" to higher solubility values at the onset of its critical behaviour. The orthoclase ($KAlSi_3O_8$) melt appears to have reached its maximum solubility near five kbars, with the lowest molar water solubility yet observed for any aluminosilicate melt. The melt with composition intermediate between SiO_2 and orthoclase (KQ: Oxtoby and Hamilton 1978b) shows a similar but slightly higher solubility than Or, at least up to around 5 kbars. From these observations, it appears that water solubility in potassium aluminosilicates is very different to that encountered in sodium aluminosilicate systems. This is supported by solubility data for melts in the system albite-orthoclase (Ab-Or) (Voigt et al. 1981; D. Voigt, personal communication 1981). At a given pressure, the molar water solubility remains almost constant between Ab and the $Ab_{25}Or_{75}$ composition, then drops sharply to almost half the albite value for Or melt. Dingwell et al. (1984) found no change in water solubility on changing the Na/K ratio from 2.23 to 1.34 in two sodium potassium aluminosil-

icate melts along the $SiO_2-(Na, K)AlSi_3O_8$ join. This could be consistent with the observation of Voigt et al. (1981), since their drop in water solubility occurred at lower Na/K ratio for the feldspar composition melts. Dingwell et al. (1984) did suggest the existence of minima in water solubility for varying Na/K ratio along lines of constant SiO_2 with $(Na+K)/Al=1$ in sodium potassium aluminosilicate melts.

Data for the system $SiO_2-CaAl_2Si_2O_8$ are also sparse, and are summarized in Fig. 8 (see also McMillan et al. 1986). The measured points for anorthite (An) melt are taken from Yoder (1965), and data for compositions along the Qz–An join were taken from Stewart (1967). In view of the large effect of silica content on water solubility in the sodium aluminosilicates, it seems surprising that addition of 28 mole% diopside component or up to 67 mole% SiO_2 to anorthite melt should have so little effect on water solubility. Solubility data for a $CaO-Al_2O_3-SiO_2$ ternary eutectic composition (E2: McMillan et al. 1986) are also shown in Fig. 8. This composition shows a solubility intermediate between $An_{33}Qz_{67}$ and $An_{80}Qz_{20}$ at near 2 kbars, but slightly higher solubility than $An_{33}Qz_{67}$ or An at 5 kbars. Finally, we have also plotted the measured points of Oxtoby and Hamilton (1978c) for melts along the Ab–An join. These show a linear increase in solubility with increasing An content which Oxtoby and Hamilton (1978c) extrapolated to give values for anorthite melt, An_{100}. However, this extrapolation gives a water solubility some 3 wt% higher than that measured by Yoder (1965). This suggests either considerable error in one or both data sets, or that water solubility exhibits a maximum between $Ab_{50}An_{50}$ and An_{100} melt.

Finally, in Fig. 9 we have summarized results of solubility determinations for a number of other aluminosilicate compositions as a function of pressure. In the system $Na_2O-Al_2O_3-SiO_2$, water solubility increases dramatically on addition of Na_2O to melts with constant Si/Al ratio (compositions Ab, 2Na, 3Na and 4Na; compositions 1.5A and Jd; Oxtoby and Hamilton 1978a, b). In fact, the 4Na melt composition (see Fig. 7) shows the highest water solubility yet observed for any aluminosilicate melt (even this measurement may represent a minimum solubility, due to the possible problems with quenching noted earlier). Within the same system, the water solubility shows a general decrease with increasing Al_2O_3 content at constant Na/Si ratio (compositions 6S, 0.5A, Ab and 1.5A (but note that the Ab and 0.5A curves cross at around 5 kbars); compositions 3Na and Ne; Oxtoby and Hamilton 1978a, b).

The above observations suggest that water solubility at both high and low pressures does show some systematic behaviour with composition for silicate and aluminosilicate melts. Below around 8 kbars, SiO_2 melt shows the lowest water solubility of all silicates or aluminosilicates, except for Or (and perhaps other potassium aluminosilicates). For binary silicates, solubility increases rapidly with increasing alkali oxide component at one atmosphere pressure, and there is some indication that this may also be the case at high pressures, at least for sodium silicate melts. Solubility also increases with decreasing silica content in CaO- and (Ca, Mg)O-silicates, but less rapidly than for the alkali silicate systems. Within the system $Na_2O-Al_2O_3-SiO_2$, water solubility increases with decreasing silica content at constant Na/Al ratio, increases dramatically with increasing Na_2O content at constant Si/Al, and decreases with increasing Al_2O_3 content at constant Na/Si. The water solubility in anorthite melt is considerably lower than that in nepheline melt, with the same Al/Si ratio, while the calcium aluminosilicate E2 (McMillan et al. 1986) which has a dry composition intermediate between the sodium aluminosilicates 2Na and 3Na (Fig. 7), has a much lower water solubility than either of these melts (Fig. 9). This could suggest that, as observed for the binary silicate systems, water solubility in calcium aluminosilicates is generally lower than that in corresponding sodium aluminosilicate melts. Potassium aluminosilicate melts along the join $SiO_2-KAlSi_3O_8$ show anomalously low solubilities, compared with binary potassi-

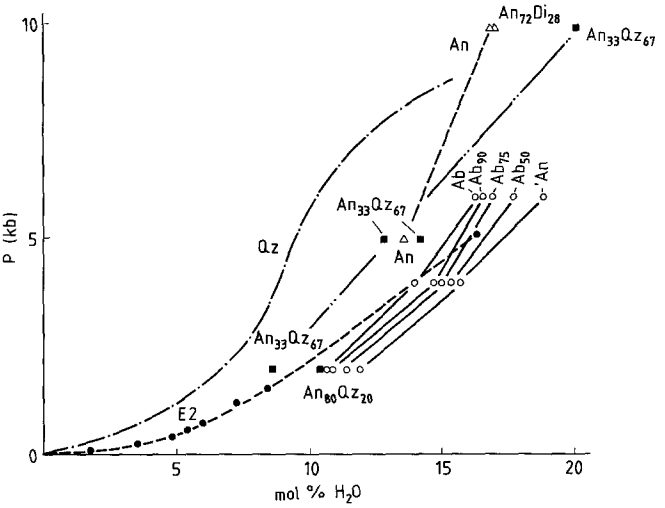

Fig. 8. Molar water solubility (one oxygen basis) in calcium aluminosilicate melts. The points for An and on the An–Di join (*open triangles*) are from Yoder (1965); the points along the Qz–An join (*filled squares*) are from Stewart (1967); points for the $CaO-Al_2O_3-SiO_2$ eutectic composition (E2) (*filled circles*) are from McMillan et al. (1986); measured points along the Ab–An join (*open circles*) are from Oxtoby and Hamilton (1978c). The points marked "An" (*open circles*) are the extrapolated values of Oxtoby and Hamilton (1978c) for An melt. The solubility curve for SiO_2 melt (Qz) from Kennedy et al. (1962) is shown for comparison

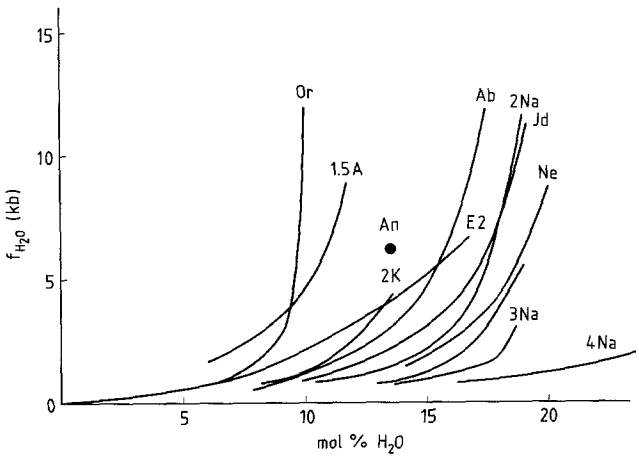

Fig. 9. Molar water solubility (one oxygen basis) in a number of aluminosilicate melt compositions. Dry melt compositions are shown in Fig. 7. Data sources are Yoder (1965) (*An*), McMillan et al. (1986) (*E2*), and Oxtoby and Hamilton (1978a, b, c) (*all other points*)

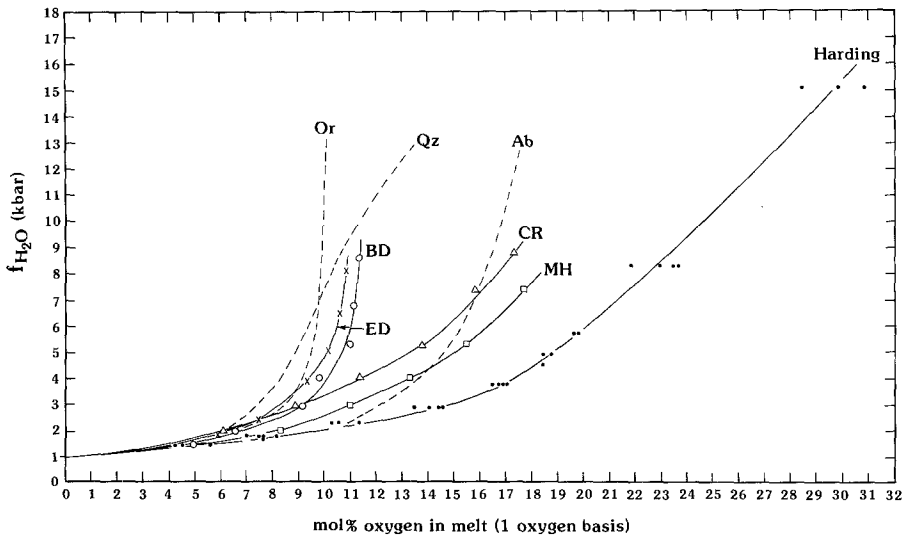

Fig. 10. Molar water solubilities (one oxygen basis) in natural melt compositions. *ED* El'Dzhurtinskii granite (Khitarov et al. 1962); *BD* Beinn an Dubhaich granite (Oxtoby and Hamilton 1978d); *HP* Harding pegmatite (Burnham and Jahns 1962); *CR* Columbia River basalt; *MH* Mount Hood andesite (Hamilton et al. 1964). Solubility curves for Qz, Or and Ab melts are shown for comparison

um silicates or sodium and calcium aluminosilicates. However, addition of K_2O to potassium aluminosilicate melts may result in a large increase in water solubility (composition 2K; Fig. 9), analogous to the increase observed for sodium aluminosilicates with constant Si/Al.

It is obvious from the limited data available that these systematics are far from complete, and can not yet be simply extrapolated from one system to another, even though the dry melts may appear similar in chemistry and properties. The identification of possible correlations of this type yields some promise of a better understanding of water dissolution mechanisms as a function of such variables as melt polymerization, Al/Si ratio, or alkali and alkaline earth metal oxide component, and also for predicting compositional variations of water solubility in natural multicomponent silicate melts. For this to be possible, many more solubility determinations as a systematic function of melt chemistry in silicate and aluminosilicate melts at both one atmosphere and high pressure will be required. Such an understanding would also provide a physical basis for constructing "realistic" thermodynamic models for hydrous aluminosilicate melts.

Natural melt compositions

The one-oxygen molar solubility curves for a number of natural melt compositions are shown in Fig. 10. These show a wide range in water solubility, probably reflecting differences in their major component melt chemistry as discussed above. The granitic compositions show the lowest molar solubility, with solubility curves comparable to those of orthoclase and quartz melts, but much lower solubilities than that of albite melt. This is an interesting observation, since these granites contain almost equal amounts of Qz, Or and Ab components in their norms (26–33%), and only minor amounts of other components. The water solubility appears however to reflect only the Or and Qz components, and not the Ab component. The Mount Hood andesite and the Columbia River basalt (Hamilton et al. 1964) compositions have much higher molar water solubilities, with andesite showing a higher solubility than basalt. Although the silica content of the andesite is higher than that of the basalt, the sodium aluminosilicate component is also slightly higher (Hamilton et al. 1964), which could partly account for the observed higher water solubility in the andesite melt. Finally, the water solubility in the Harding pegmatite composition (Burnham and Jahns 1962) is very much higher than any of these compositions, which has been suggested is associated with the high Li or Rb content of the pegmatite (Oxtoby and Hamilton 1978d; Dingwell et al. 1984). However, in view of the effects of temperature discussed earlier, this could also be due to the lower temperatures of the solubility experiments of this composition (Burnham and Jahns 1962).

The mechanism of water dissolution

Probably the simplest model proposed for the dissolution of water in silicate melts is via reaction of H_2O with oxygen in the melt to give two $-OH$ groups. Mechanisms of this type are frequently encountered in both the glass science and the geological literature (e.g., Tomlinson 1956; Russell 1957; Scholze 1966; Hamilton et al. 1964; Mysen 1977; Eggler and Rosenhauer 1978; Oxtoby and Hamilton 1978a). However a number of workers at various times have argued for some proportion of molecular (i.e., undissociated) H_2O as a dissolving species in the melt or glass (e.g., Orlova 1962; Scholze 1966; Hodges 1974). More recently, Stolper (1982a, b) has reviewed the problem and carried out a systematic series of quantitative infra-red absorption studies on natural and synthetic aluminosilicate glasses quenched from hydrous melts. This work showed that, at low water contents, a dissolution mechanism involving only hydroxyl ($-OH$) groups was a good approximation, but that at higher water contents, both hydroxyl and molecular H_2O groups were present in the hydrous glasses. The ratio of molecular water to hydroxyl groups increased rapidly with increasing water content. Stolper (1982a, b) further showed that the molecular H_2O was not simply present as submicroscopic bubbles of trapped fluid, but should be considered as a true dissolving species in the melt. Stolper and co-workers have since extended their observations to higher pressures and temperatures to above the glass transition (Stolper et al. 1983; Aines et al. 1983), indicating that the observed speciation of hydrous components, and the derived water dissolution model, may be applied to the corresponding hydrous melts at geological pressures and temperatures.

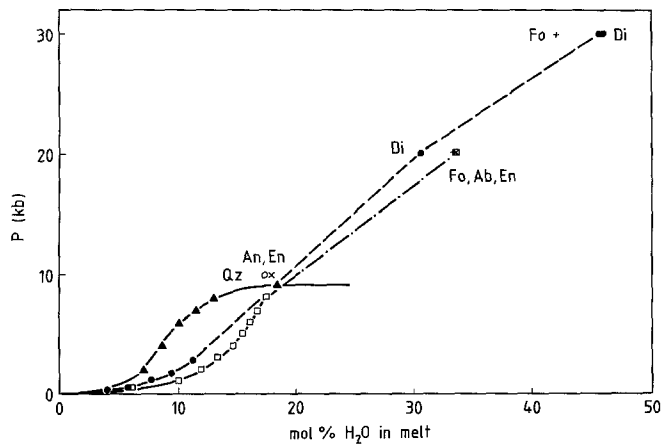

Fig. 11. Molar water solubilities (one oxygen basis) for aluminosilicate melts at high pressures. Data sources: *Qz* (Kennedy et al. 1962); *An* (Yoder 1965); *Ab*, *Di* (Eggler 1973); *Fo* (Hodges 1973, 1974); *En* (Eggler 1973; Kushiro and Yoder 1968)

Stolper (1982a) noted that, since water solubility at high pressure would be dominated by solvation of molecular H_2O as the dissolution mechanism, there should be little compositional dependence of water solubility at high pressures. This seems to be borne out by the few water solubility experiments at pressures above 20 kbars (Fig. 11). This might also correlate with the observed difficulty of quenching hydrous melts with high water contents (Kadik and Lebedev 1968). While water solubility shows a strong compositional dependence in the 1–10 kbar range (Figs. 5, 6, 8, 9), such widely different compositions as Fo, Di, Ab, An and En melts show solubilities which are within 10% of each other above around ten kilobars (Fig. 11).

Supercritical behaviour

Kennedy et al. (1962) have described the upper critical behaviour of the system SiO_2-H_2O, with complete mutual solubility in the fluid phase above around ten kbars at near 1000° C. This behaviour has never been reported for more complex silicate or aluminosilicate compositions, although Kennedy et al. (1962) suggested that it might occur in the $SiO_2-KAlSi_3O_8-NaAlSi_3O_8$ system. Goldsmith and Jenkins (1985) have recently studied the hydrothermal melting of albite to around 20 kbars. These authors noted that, above 14 kbars, the melting curves for both high and low albite showed a "distinct flattening of the dP/dT slope", and the quenched melt product consisted of "a soft powder, amorphous to X-rays" (Goldsmith and Jenkins 1985). On analysis by scanning electron microscopy, this powder consisted of rounded globules 2–5 microns in diameter. It is possible that these globules could represent aluminosilicate component which had been dissolved in the aqueous fluid at high pressure and temperature and deposited on quenching, i.e., that the albite-water system had become supercritical above around 14 kbars and several hundred degrees Celsius. As noted earlier, the low temperature solubility curve of Burnham and Jahns (1962) for albite melt showed a distinct flattening to higher solubility values above around 5–7 kbars which could indicate the onset of supercritical behaviour (Fig. 2). Water solubility data both at low and high pressures (above and below around 10 kbars) for Ab and Di melts at higher temperature (Eggler 1973; Rosenhauer and Eggler 1975; Eggler and Rosenhauer 1978; Oxtoby and Hamilton 1978a, b) are shown in Fig. 11. If the solubility curves below 10 kbars are extrapolated to the high pressure values, the curves must bend strongly to higher solubilities to reach the 20 and 30 kbar points. Again, this is reminiscent of the critical behaviour observed for SiO_2 (Fig. 11), and would indicate mutual solubility in the fluid at high pressure for the systems $Ab-H_2O$ and $Di-H_2O$. If so, it is unlikely that the multicomponent silicate and aluminosilicate compositions would approach the critical region along a congruent line of mixing, due to differential dissolution of melt components in the fluid. Anderson and Burnham (1983) have discussed the importance and nature of the solubility of melt components in the aqueous fluid for feldspar compositions at lower pressures.

Spectroscopic experiments

The work of Stolper (1982a, b) has shed much light on the general nature of water dissolution in silicate melts, but does not account for the observed strong compositional dependence of water solubility over much of the pressure range. At present, there is little further information regarding the speciation of hydroxyl groups in hydrous silicate glasses or melts.

Hydrous aluminosilicate glasses show an infrared band near 4500 cm^{-1}, arising from the combination of O–H stretching vibrations near 3600 cm^{-1} with Si–OH and/or Al–OH vibrations in the 900–1000 cm^{-1}. The 4500 cm^{-1} band is thus due to hydroxyl groups attached to Si and/or Al in the glass (Fig. 12a; Stolper 1982a). A second band at 5200 cm^{-1} is due to the combination of O–H stretching with the HOH bending vibration near 1600 cm^{-1}, and is then due to molecular H_2O groups in the glass or melt (Stolper 1982a). For a variety of hydrous aluminosilicate melts, Stolper (1982a, b) consistently obtained the correct total water content (measured independently) for the glass sample by summing the contributions from the molecular water signal at 5200 cm^{-1} and the 4500 cm^{-1} band. This suggests that within experimental error, all hydroxyl groups in the glass are associated with either Si or Al, or both. This is an important result, and suggests that the Na–OH species inferred by Mysen and Virgo (1986a, b) are not necessary to explain the solubility data.

Even for the simplest hydrous silicate and aluminosilicate glasses, detailed assignment of structural species remains problematic. Hydrous SiO_2 glasses show a Raman and infrared peak at 970 cm^{-1} (Fig. 12b) which has been assigned to the stretching vibration of silanol (SiOH) groups (Hartwig and Rahn 1977; McMillan and Remmele 1986). Huffman and McMillan (1985) observed a peak at 885 cm^{-1} in the Raman spectrum of hydrated amorphous SiO_2 samples, which could correspond to silicate tetrahedra with two OH groups, $=Si(OH)_2$. No such peak has been observed in the spectra of hydrous SiO_2 glasses quenched from the melt. However, Mysen and Virgo (1982a) have suggested the presence of a second component in a deconvolution of the 970 cm^{-1} peak of SiO_2 glass with 5–10 wt% water. Although Mysen and Virgo (1986a) suggest that this component lies near 960 cm^{-1}, it is also possible that the broadening at the base of the 970 cm^{-1} band is due to a feature near 890 cm^{-1}. McMillan and Remmele (1986) and Mysen and Virgo (1986a) have observed a peak at

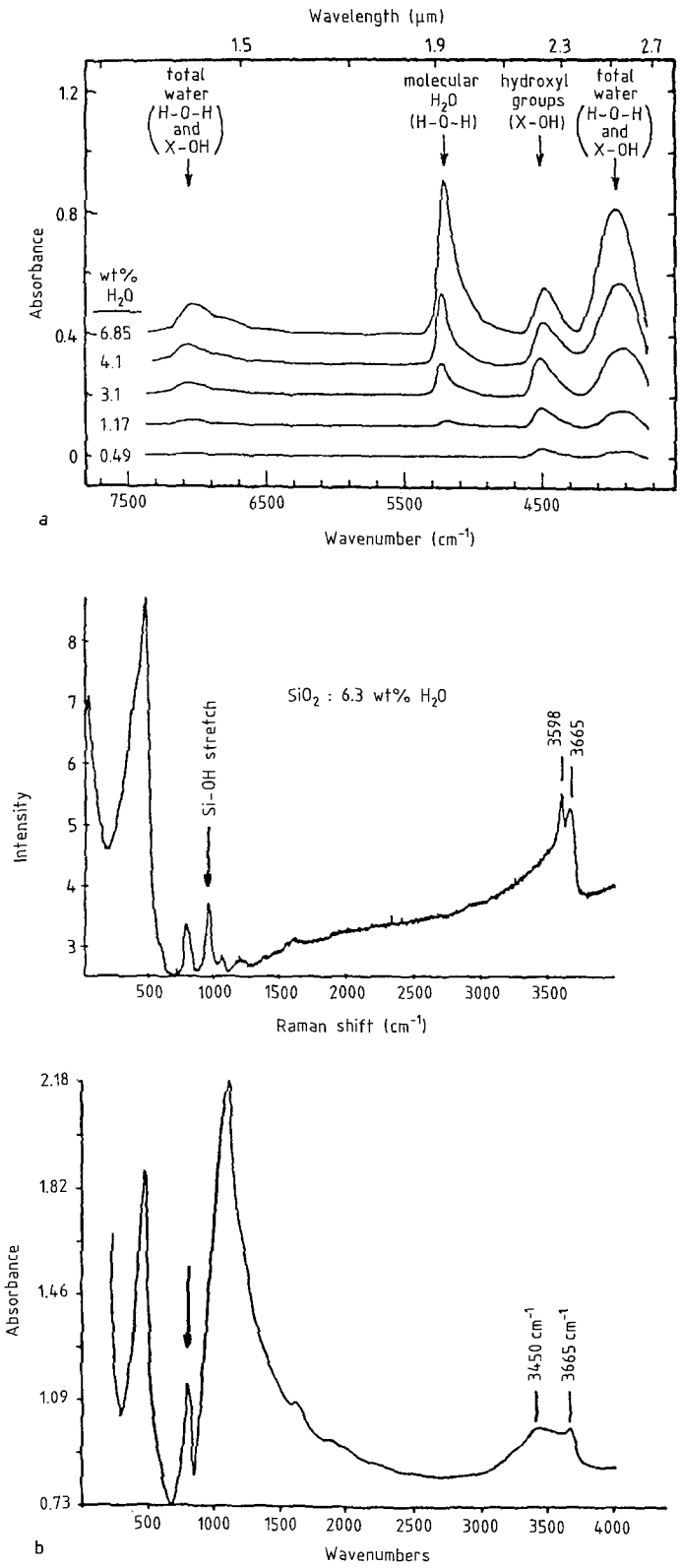

Fig. 12. a Near infrared absorbance spectra for hydrous aluminosilicate glasses with variable water contents, from Stolper (1982b). These spectra show the peaks near 5260 cm^{-1} (1.9 μ) due to combination of O–H stretching and HOH bending vibrations of molecular H_2O, and near 4550 cm^{-1} (2.2 μ) due to combination of O–H stretching and (Si, Al)–OH stretching or bending. **b** Raman (*top*) and infrared (*bottom*) spectra of SiO_2 glass containing 6.3 wt% water. The peak near 970 cm^{-1} is due to Si–OH stretching (McMillan and Remmele 1986)

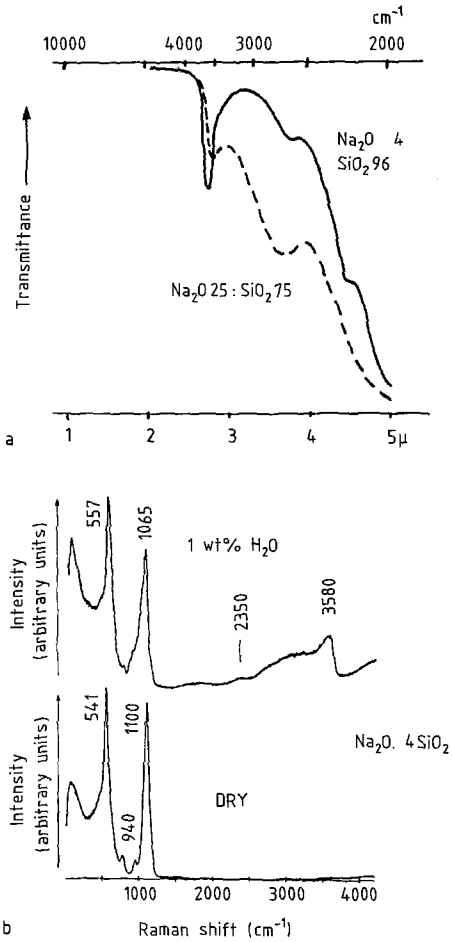

Fig. 13. a Infrared spectra of sodium silicate glasses containing approximately 0.03 wt% water from Scholze (1966), showing the band near 2780 cm^{-1} (3.6 μ) suggested to be associated with OH stretching vibrations involved in hydrogen bonding. **b** Raman spectrum of a sodium silicate glass containing approximately 1 wt% water from McMillan and Remmele (1986) showing the 2350 cm^{-1} band suggested to be associated with O–H stretching vibrations involved in intra-molecular H-bonding

3598 cm^{-1} in the O–H stretching region of the Raman spectrum for SiO_2 glass which grows in intensity with increasing water content (Fig. 12b). This peak remains unexplained, but certainly corresponds to some new hydroxyl species appearing at high water content in SiO_2 glass, and perhaps in the hydrous melt.

Scholze and coworkers (Scholze and Franz 1962; Scholze 1966) have observed a band near 2800 cm^{-1} (Fig. 13a) in the infrared spectra of a number of binary silicate glasses $SiO_2-M_2O-M'O$ (M=Li, Na, K; M'= Ca, Ba), which they associated with stretching of OH groups involved in hydrogen bonding. McMillan and Remmele (1986) also observed a weak band near 2350 cm^{-1} in the Raman spectrum of a hydrous sodium silicate glass (Fig. 13b), which they interpreted as O–H stretching of SiOH groups involved in intramolecular hydrogen bonding, presumably to non-bridging oxygens within depolymerized silicate units. If these assignments are correct, they could help rationalize the observed increase in water solubility with decreasing silica content in binary silicate melts, through increased stabilization of hydroxylated species via

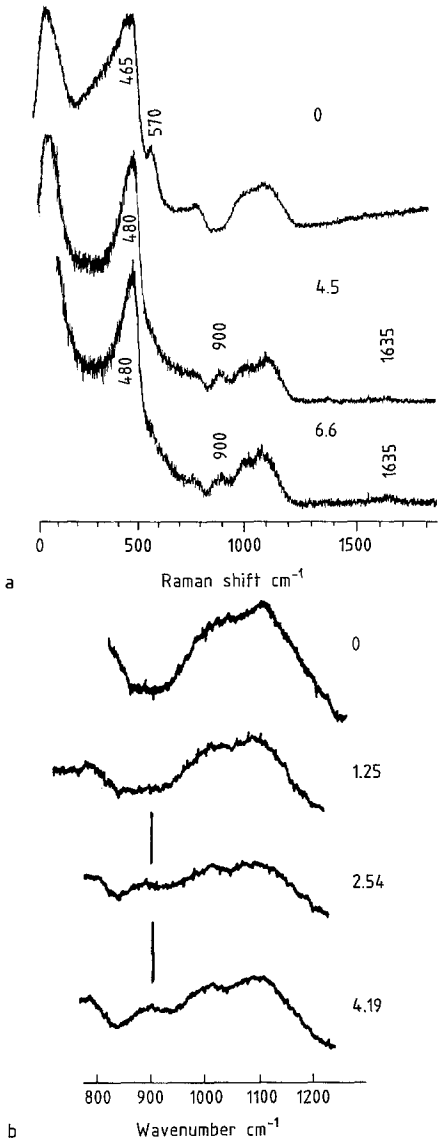

Fig. 14a, b. Raman spectra of hydrous albite glasses with variable water content from (**a**) McMillan et al. (1983) and (**b**) Mysen et al. (1980). The water contents are shown in wt% to the right of the Figure. Remmele et al. (1986) suggest that the 900 cm^{-1} band is due to Al–OH vibrations, while Mysen and Virgo (1982) and Mysen (1983) consider that it is not due to hydrous species in the glass

hydrogen bonding interactions. However, these arguments do not explain the observed differences in water solubility between alkali silicate melts and corresponding alkaline earth silicate melts.

The Raman spectra of hydrous aluminosilicate glasses show a new peak at 900 cm^{-1} which increases in intensity with water content (Fig. 14: Mysen et al. 1980; McMillan et al. 1984). Mysen et al. (1980) and Mysen and Virgo (1982) concluded that this peak showed no H/D isotope shift, hence could not be due to a vibration involving Al–OH or any other hydrogen-bearing species. However, Remmele et al. (1986) have observed a small but reproducible H/D isotope effect for the 900 cm^{-1} peak in several hydrous sodium aluminosilicate glasses, and concluded that the peak was in fact due to hydrous species. Remmele et al. (1986) further suggested that the 900 cm^{-1} peak was associated with AlOH species in the hydrous aluminosilicate glasses. There was no evidence for a 970 cm^{-1} peak in any of the hydrous aluminosilicate glasses studied by these workers, suggesting that no Si–OH groups are formed in the hydrous melt (Mysen and Virgo 1986a, b; Remmele et al. 1986). If the interpretation of Remmele et al. (1986) is realistic, this would imply that Al–OH groups are formed preferentially in hydrous aluminosilicate melts, presumably accompanied by a redistribution of SiOSi, SiOAl and AlOAl linkages. If this were the case, that H_2O reacts preferentially with aluminium in aluminosilicate melts, this would be consistent with the observed stability of hydrous alumina and aluminate phases, and could rationalize the observed increase in water solubility with decreasing silica content within the Qz–Ne series. However, this rationalization can not be applied to the potassium aluminosilicate melts along the Qz–Or join, which show much lower solubilities, and do not show any simple relation between silica content and water solubility. It is obvious that further work is needed to clarify these important points.

Conclusion

From the discussion in this paper, it is obvious that there is already a large data base on water solubility in aluminosilicate melts, but there are many gaps in the data, and some should be re-measured to eliminate errors due to experimental technique. The data available show some underlying systematics, but more solubility measurements must be made before regular compositional variations may be recognized. The correlations we have found suggest that the physical geochemistry of hydrous aluminosilicate melts is complex and fascinating, and that our understanding of water dissolution is only beginning. The interaction between water and silicate melts at high pressures and temperatures remains one of the central problems in geochemistry, and deserves a serious and systematic study.

Acknowledgements. Much of the time during compilation of these data was supported by NSF grant EAR-7809954 to J. Holloway, while P. McMillan acknowledges support from NSF grant EAR-8407105. We are grateful to D. Hamilton for kindly providing unpublished solubility data obtained by S. Oxtoby, and allowing us to refer to the data in this work. Finally, we thank J. Stebbins and D. Eggler for the time they spent in providing thoughtful and constructive reviews.

References

Aines RD, Silver LA, Rossman GR, Stolper EM, Holloway JR (1983) Direct observation of water speciation in rhyolite at temperatures up to 850° C. Geol Soc Am Abstr Prog 15:512

Anderson GM, Burnham CW (1983) Feldspar solubility and the transport of aluminum under metamorphic conditions. Am J Sci 283A:283–297

Burnham CW (1974) $NaAlSi_3O_8-H_2O$ solutions: a thermodynamic model for hydrous magmas. Bull Soc Fr Mineral Cristallogr 97:223–230

Burnham CW (1975a) Water and magmas: a mixing model. Geochim Cosmochim Acta 39:1077–1084

Burnham CW (1975b) Thermodynamics of melting in experimental silicate-volatile systems. Fortschr Mineral 52:101–118

Burnham CW (1979) The importance of volatile constituents. In: Yoder HS (ed) The evolution of the igneous rocks: fiftieth anniversary perspectives. Princeton Univ Press, pp 439–482

Burnham CW (1981) The nature of multicomponent silicate melts. In: Rickard DT, Wickman FE (eds) Chemistry and geochemistry at high temperatures and pressures: Physics and chemistry of the earth, vols. 13 and 14, pp 197–229

Burnham CW, Davis NF (1971) The role of H_2O in silicate melts I. P–V–T relations in the system $NaAlSi_3O_8-H_2O$ to 10 kilobars and 1000° C. Am J Sci 270:54–79

Burnham CW, Davis NF (1974) The role of H_2O in silicate melts: II. Thermodynamic and phase relations in the system $NaAlSi_3O_8-H_2O$ to 10 kbars, 700° to 1000° C. Am J Sci 274: 902–940

Burnham CW, Jahns RH (1962) A method for determining the solubility of water in silicate melts. Am J Sci 260:721–745

Burnham CW, Nevkasil H (1986) Equilibrium properties of granite pegmatite magmas. Am Mineral 71:239–263

Coutures JP, Peraudeau G (1981) Examen de la dissolution de l'eau dans les silicates liquides [$P(H_2O) \leq 1$ atm]. Rev Int Hautes Temp Refract 18:321–346

Coutures JP, Devauchelle JM, Munoz R, Urbain G (1980) Dissolution of water vapor in $SiO_2-Al_2O_3$ melts. Rev Int Hautes Temp Refract 17:351–361

Devauchelle JM (1978) Contribution a l'étude de la dissolution de la vapeur d'eau dans les silicates liquides. Thesis, Université de Perpignan

Dingwell DB, Harris DM, Scarfe CM (1984) The solubility of H_2O in melts in the system $SiO_2-Al_2O_3-Na_2O-K_2O$ at 1 to 2 kbars. J Geol 92:387–395

Eggler DH (1973) Role of CO_2 in melting processes in the mantle. Carnegie Inst Wash Yearb 72:457–467

Eggler DH and Burnham CW (1984) Solution of H_2O in diopside melts: a thermodynamic model. Contrib Mineral Petrol 85:58–66

Eggler DH, Rosenhauer M (1978) Carbon dioxide in silicate melts. II. Solubilities of CO_2 and H_2O in $CaMgSi_2O_6$ (diopside) liquids and vapors at pressures to 40 kb. Am J Sci 278: 64–94

Goldsmith JR, Jenkins D (1985) The hydrothermal melting of low and high albite. Am Mineral 70:924–945

Goranson RW (1931) The solubility of water in granitic magmas. Am J Sci 22:481–502

Goranson RW (1937) The osmotic pressure of silicate melts: Am Mineral 22:485

Hamilton DL, Oxtoby S (1986) Solubility of water in albite melt determined by the weight-loss method. J Geol 94:626–630

Hamilton DL, Burnham CW, Osborn EF (1964) The solubility of water and effects of oxygen fugacity and water content on crystallization in mafic magmas. J Petrol 5:21–39

Hartwig CM, Rahn LA (1977) Bound hydroxyl in vitreous silica. J Chem Phys 67:4260–4261

Hodges FN (1973) Solubility of H_2O in forsterite melt at 20 kbar. Carnegie Inst Washington Yearb 72:495–497

Hodges FN (1974) The solubility of H_2O in silicate melts: Carnegie Inst Wash Yearb 73:251–255

Huffman M, McMillan P (1985) Infrared and Raman studies of chemically vapor deposited amorphous silica. J Non-Cryst Solids 76:369–379

Iguchi Y, Fuwa T (1970) Solubility of water in liquid $CaO-SiO_2-MgO$ with and without FeO at 1550 degrees C. Trans Iron Steel Inst Jpn 10:29–35

Iguchi Y, Ban-Ya S, Fuwa T (1969) Solubility of water in liquid $CaO-SiO_2$ with Al_2O_3, TiO_2 and FeO at 1550° C. Trans Iron Steel Inst Jpn 9:189–195

Kadik AA, Lebedev YeB (1968) Temperature dependence of the solubility of water in an albite melt at high pressures. Geochimica 12:1172–1181 (original Geokhimiya 12:1444–1455)

Karsten JL, Holloway JR, Delaney JR (1982) Ion microprobe studies of water in silicate melts: temperature-dependent water diffusion in obsidian. Earth Planet Sci Lett 59:420–428

Kennedy GC, Wasserburg GJ, Heard HC, Newton RC (1962) The upper three-phase region in the system SiO_2-H_2O. Am J Sci 260:501–521

Kurkjian CR, Russell LE (1958) Solubility of water in molten alkali silicates. J Soc Glass Technol 42:130T–144T

Kushiro I, Yoder HS (1968) Silicate systems including a vapor phase. Melting of forsterite and enstatite at high pressures under hydrous conditions. Carnegie Inst Washington Yearb 67:153–167

McMillan P (1984) Structural studies of silicate glasses and melts-applications and limitations of Raman spectroscopy. Am Mineral 69:622–644

McMillan P, Holloway JR (1983) Water dissolution in silicate melts (abstr). EOS 64:339

McMillan PF, Remmele RL (1986) Hydroxyl sites in SiO_2 glass: a note on infrared and Raman spectra. Am Mineral 71: 772–778

McMillan PF, Jakobsson S, Holloway JR, Silver L (1983) A note on the Raman spectra of water-bearing albite glasses. Geochim Cosmochim Acta 47:1937–1943

McMillan PF, Peraudeau G, Holloway JR, Coutures JP (1986) Water solubility in a calcium aluminosilicate melt. Contr Mineral Petrol 94:178–182

Mysen BO (1977) The solubility of H_2O and CO_2 under predicted magma genesis conditions and some petrological and geophysical implications. Rev Geophys Space Phys 15:351–361

Mysen BO (1983) The solubility mechanisms of volatiles in silicate melts and their relations to crystal-andesite liquid equilibria. J Volcanol Geotherm Res 18:361–385

Mysen BO, Virgo D (1980) Solubility mechanisms of water in basalt melt at high pressures and temperatures: $NaCaAlSi_2O_7-H_2O$ as a model. Am Mineral 65:1176–1184

Mysen BO, Virgo D (1982) Solubility mechanisms of H_2O in silicate melts at high pressures and temperatures: a Raman spectroscopic study: reply. Am Mineral 67:155

Mysen BO, Virgo D (1986a) Volatiles in silicate melts at high pressure and temperature. 1. Interaction between OH groups and Si^{4+}, Al^{3+}, Ca^{2+}, Na^+ and H^+. Chem Geol 57:303–331

Mysen BO, Virgo D (1986b) Volatiles in silicate melts at high pressure and temperature. 2. Water in melts along the join $NaAlO_2-SiO_2$ and a comparison of solubility mechanisms of water and fluorine. Chem Geol 57:333–358

Mysen BO, Virgo D, Harrison WJ, Scarfe CM (1980) Solubility mechanisms of H_2O in silicate melts at high pressures and temperatures: a Raman spectroscopic study. Am Mineral 65:900–914

Orlova GP (1962) The solubility of water in albite melts. Int Geol Rev 6:254–258

Orlowski HJ, Koenig CJ (1941) Thermal expansion of silicate fluxes in the crystalline and glassy states. Am Ceram Soc Bull 24:80–84

Oxtoby S, Hamilton DL (1978a) The discrete association of water with Na_2O and SiO_2 in NaAl silicate melts. Contrib Mineral Petrol 66:185–188

Oxtoby S, Hamilton D (1978b) Solubility of water in melts of the $Na_2O-Al_2O_3-SiO_2$ and $K_2O-Al_2O_3-SiO_2$ systems. In: Mackenzie WS (ed) Progress in experimental petrology. Natl Environ Res Council Pub Ser D No 11. Dept of Geology Manchester Univ, pp 33–36

Oxtoby S, Hamilton D (1978c) Water in plagioclase melts. In: Mackenzie WS (ed) Progress in experimental petrology. Natl Environ Res Council Pub Ser D No 11. Dept of Geology, Manchester Univ, pp 36–37

Oxtoby S, Hamilton D (1978d) Calculation of the solubility of water in granitic melts. In: Mackenzie WS (ed) Progress in experimental petrology. Natl Environ Res Council Pub Ser D No 11. Dept of Geology, Manchester Univ, pp 37–40

Remmele R, Stanton T, McMillan P, Holloway J (1986) Raman spectra of hydrous glasses along the quartz-albite join (abstr). EOS 67:1274

Rosenhauer M, Eggler DH (1975) Solution of H_2O and CO_2 in diopside melt. Carnegie Inst Wash Yearb 74:474–479

Russell LE (1957) Solubility of water in molten glass. J Soc Glass Technol 41:304T–317T

Sachdev PL, Majdic A, Schenck H (1972) Solubility of water in lime-alumina-silica melts. Metall Trans 3:1537–1543

Scholze H (1966) Gases and water in glass: Parts one, two and three. The Glass Industry. Part one pp 546–551, Part two pp 622–628, Part three pp 670–674

Scholze H, Franz H (1962) Zur Frage der IR-Bande bei 4,25 μ in Gläsern. Glastech Ber 35:278–281

Scholze H, Mulfinger HO, Franz H (1962) Measurement of the physical and chemical solubility of gases in glass melts (He and H_2O). In Advances in glass technology, Technical papers of VI Int Congress on Glass, compiled by Am Ceram Soc. Plenum Press, pp 230–248

Silver L, Stolper E (1985) A thermodynamic model for hydrous silicate melts. J Geol 93:161–177

Stewart DB (1967) Four-phase curve in the system CaAl2Si208 – $SiO_2 - H_2O$ between 1 and 10 kilobars. Schweiz Mineral Petrol Mitt 47:35–59

Stolper E (1982a) The speciation of water in silicate melts. Geochim Cosmochim Acta 46:2609–2620

Stolper E (1982b) Water in silicate glasses: an infrared spectroscopic study. Contrib Mineral Petrol 81:1–17

Stolper E, Silver LA, Aines RD (1983) The effects of quenching rate and temperature on the speciation of water in silicate glasses (abstr). EOS 65:339

Tomlinson JW (1956) A note on the solubility of water in molten sodium silicate. J Soc Glass Technol 4:25T–31T

Tuttle OF, Bowen NL (1958) Origin of granite in the light of experimental studies in the system $NaAlSi_3O_8 - KAlSi_3O_8 - SiO_2 - H_2O$. Geol Soc Am Mem 74

Uys JM, King TB (1963) The effect of basicity on the solubility of water in silicate melts. Trans Metall Soc AIME 227:492–500

Voigt DE, Bodnar RJ, Blencoe JG (1981) Water solubility in melts of alkali feldspar composition at 5 kbar, 950° C. EOS 62:428

Walsh JH, Chipman J, King TB, Grant NJ (1956) Hydrogen in steelmaking slags. J Met 206:1568–1576

Wasserburg GJ (1957) The effects of H_2O in silicate systems J Geol 65:15–23

Yoder HS (1965) Diopside-anorthite-water at five and ten kilobars and its bearing on explosive volcanism. Carnegie Inst Washington Yearb 64:82–89

Received December 15, 1986 / Accepted July 7, 1987